Radiat Environ Biophys (2016) 55:53–59
DOI 10.1007/s00411-015-0628-z

ORIGINAL ARTICLE

In vitro RABiT measurement of dose rate effects on radiation induction of micronuclei in human peripheral blood lymphocytes

Antonella Bertucci[1] · Lubomir B. Smilenov[1] · Helen C. Turner[1] · Sally A. Amundson[1] · David J. Brenner[1]

Received: 5 January 2015 / Accepted: 28 November 2015 / Published online: 20 January 2016

Abstract Developing new methods for radiation biodosimetry has been identified as a high-priority need in case of a radiological accident or nuclear terrorist attacks. A large-scale radiological incident would result in an immediate critical need to assess the radiation doses received by thousands of individuals. Casualties will be exposed to different doses and dose rates due to their geographical position and sheltering conditions, and dose rate is one of the principal factors that determine the biological consequences of a given absorbed dose. In these scenarios, high-throughput platforms are required to identify the biological dose in a large number of exposed individuals for clinical monitoring and medical treatment. The Rapid Automated Biodosimetry Tool (RABiT) is designed to be completely automated from the input of blood sample into the machine to the output of a dose estimate. The primary goal of this paper was to quantify the dose rate effects for RABiT-measured micronuclei in vitro in human lymphocytes. Blood samples from healthy volunteers were exposed in vitro to different doses of X-rays to acute and protracted doses over a period up to 24 h. The acute dose was delivered at $\sim$1.03 Gy/min and the low dose rate exposure at $\sim$0.31 Gy/min. The results showed that the yield of micronuclei decreases with decreasing dose rate starting at 2 Gy, whereas response was indistinguishable from that of acute exposure in the low dose region, up to 0.5 Gy. The results showed a linear-quadratic dose–response relationship for the occurrence of micronuclei for the acute exposure and a linear dose–response relationship for the low dose rate exposure.

Keywords Biodosimetry · Micronuclei · RABiT · High throughput · Nuclear accident

Introduction

The development of improved methods for radiation biodosimetry has been identified as a high-priority need in an environment of heightened concern over possible radiological or nuclear terrorist attacks (Pellmar et al. 2005; Kulka et al. 2015). The detonation of even a small radioactive dispersal device (RDD) in a large metropolitan area would be likely to create large-scale panic, despite the low risk of radiological injuries. A small improvised nuclear device (IND) would produce a major health emergency in addition to mass panic. In such situations, in that the general population would not be carrying physical dosimeters, a very high throughput means of assessing the radiation exposure based on biological endpoints will be needed. This will serve to reduce panic by both reassuring those who were not significantly exposed and triaging those in need of medical attention (Garty et al. 2010).

When planning for the response to an IND detonation, it is assumed that radiation exposure will occur through two pathways: prompt radiation near the site of the detonation, which gives off radiation at a high dose rate, and residual radiation (fallout), which has a lower dose rate. Therefore, these scenarios involve significant components of the dose being delivered over many hours. Also, the total absorbed dose is dependent on location and duration of exposure. Sheltering on-site during the initial phase (hours to 1 day) can considerably reduce exposure (Knebel et al. 2011).

✉ Antonella Bertucci
bertucci.antonella@gmail.com

[1] Center for Radiological Research, Columbia University Medical Center, 630 W. 168th St., New York, NY 10032, USA

There will be the "Dangerous Fallout Zone" (DFZ) in which victims will be at risk of acute radiation syndrome (ARS), and this zone will reach its maximum extent after the first few hours and then shrink in size in just 1 day (DiCarlo et al. 2011).

Computer models indicate that within about 24 h of a 10-KT IND detonation, the most significant fallout hazard area will extend 10–20 miles from ground zero. Within a few miles of ground zero, exposure rates in excess of 100 R/h during the first 4–6 h post-detonation may be observed; 24 h post-detonation, the estimated dose rate in the same conditions will reach a value of ~0.38 cGy/min. The NCRP recommend defining the perimeter of the DFZ as an area with an exposure rate of 10 R/h (~0.1 Gy h-1 air-kerma rate). In a DFZ, external exposure to gamma radiation is the dominant health concern; however, β radiation can cause severe tissue damage when fallout material remains in contact with unprotected skin.

Casualties inside the DF zone will be exposed to different dose rates due to their geographical position and sheltering conditions. Dose rate is one of the principal factors that determine the biological consequences of a given absorbed dose (Hall 1991; Vilenchik and Knudson 2006; Turesson 1990). As the dose rate is lowered and the exposure time extended, the biological effect of a given dose generally is reduced (Knebel et al. 2011). It is well known that the dose rate effect must be considered when evaluating risks since many studies reported a significant biological reduced response with decrease in the dose rate (DiCarlo et al. 2011).

Among the casualties of an IND, thousands of persons would be exposed to radioactive fallout downwind from the explosion. Such victims might be exposed to substantial doses of radiation, but without clear signs and symptoms of radiation toxicity or exposure initially. There is thus a need for rapid, accurate and sensitive diagnostic platforms that can confirm exposure and estimate the radiation dose absorbed (Ramakrishnana and Brenner 2008).

In large-scale events such as an IND, rapid tools are required to identify the physical dose individuals were exposed to in order to provide appropriate clinical monitoring and treatment (Jaworska et al. 2015). The principle of biodosimetry is to utilize changes induced in the individuals by ionizing radiation to estimate the dose and, if possible, to predict or reflect the clinically relevant dose. Emerging biodosimetric techniques utilize changes in tissues of individuals exposed to ionizing radiation as a quantitative measure of the absorbed dose (Swartz et al. 2014). Several recent approaches for biodosimetry include biological response to ionizing radiation through gene expression (Paul and Amundson 2008) protein products (Marchetti et al. 2006) or measures of products of altered metabolism (Laiakis et al. 2014; Goudarzi et al. 2014a, b; Coy et al. 2011). However, more mature assays, such as the dicentric chromosome assay (DCA) and the cytokinesis-block micronucleus assay (CBMN) in peripheral blood lymphocytes (PBL), have been extensively validated as biodosimeters for dose estimation purposes (Padovani et al. 1993; Thierens et al. 2005; 2014; Voisin et al. 2001; 2004; Fenech 2010; Rothkamm et al. 2013).

Compared to the DCA, considered the "gold standard" for biological dosimetry, the CBMN is characterized by very easy and rapid scoring. This feature in addition to its good reliability and reproducibility (Fenech 2006) makes this method very attractive for large-scale assessment of genetic damage in radiation workers (Thierens et al. 2005) and for population triage in case of a large-scale radiation accident (Thierens and Vral 2009). Several reports have demonstrated that the CBMN assay can detect dose rate effects in micronuclei (MNi) yields, namely a decrease with decreasing dose rate, reflecting increased repair (Bhat and Rao 2003; Boreham et al. 2000; Sorensen et al. 2000).

Following a large-scale radiological event, the first responders will be able to reach the location of the accident in a few hours after the initial event (Pellmar et al. 2005). It is estimated that the earliest organized emergency response will be capable of collecting samples for an initial victim triage of the accident in not less than 24 h post-event (Pellmar et al. 2005; DiCarlo et al. 2011). These collection sites will require advanced high-throughput biodosimetry platforms (Knebel et al. 2011). Over the past years, our group has developed such a platform, the Rapid Automated Biodosimetry Tool (RABiT). The RABiT completely automates three well-established biodosimetry assays: the CBMN (Fenech 2007; Lyulko et al. 2014), the yield of phosphorylation of the histone H2AX (γ-H2AX assay; Redon et al. 2009; Turner et al. 2011; Garty et al. 2015) and the dicentric assay (Repin et al. 2014). The RABiT allows high-throughput analysis of thousands of blood samples per day, providing a dose estimate of past radiation exposure that can be used to support clinical triage and treatment decisions (Garty et al. 2011).

The primary goal of this paper was to quantify the dose rate effects for RABIT-measured micronuclei in vitro in human lymphocytes. For the MNi assay, studies aimed at characterizing the dose rate effect for radiation-induced micronuclei in human lymphocytes showed that the MNi yield decreases with decreasing dose rate (Bhat and Rao 2003; Sorensen et al. 2000; Geard and Chen 1990; Scott et al. 1996). Furthermore, it has been demonstrated that the MNi response curve in human peripheral lymphocytes decreased with decreasing dose rate, becoming more curvilinear, with a pure linear response of MNi induction observed at lowest dose rate (Bhat and Rao 2003). However, all these studies were performed with the standard CBMN, in which blood samples exposed to ionizing

radiation are processed immediately or in a short period of time (from minutes to a few hours) after irradiation.

In addition to our primary goal, we measure in a realistic scenario, how the RABiT-measured micronuclei yield in human lymphocytes changes with exposure time, over periods of up to 24 h, compared to acute (few seconds) exposure. Furthermore, in order to validate the RABiT-measured micronuclei frequencies 24 h post-irradiation, we compared the results obtained with micronuclei frequencies measured in blood samples exposed with the same ADR modalities and doses and processed in the standard CBMN assay (within 1 h post-irradiation).

Materials and methods

Experimental design

Our main assumption is that following a large-scale radiological event the first responders will be able to reach the location of the accident after 24 h post-irradiation. Therefore, the experimental design selected for this study considers that blood samples will be obtained 24 h post-detonation from victims who have been exposed to a variety of dose rates and doses. Those individuals who were close to the explosion area would be exposed to high doses of radiation at a high dose rate (ADR). Conversely, people who were located a certain distance from the source of radiation or who were shielded (e.g., those inside buildings) would be exposed with a low dose rate modality (LDR).

Human blood was exposed in vitro to different acute and protracted doses of X-rays over a period of 24 h. The acute dose rate (ADR) exposure was delivered at $\sim$1.03 Gy/min and the low dose rate (LDR) exposure at $\sim$0.31 cGy/min. Assuming that in a realistic scenario the earliest samples could be collected would be 24 h post-irradiation, MNi frequencies were measured in vitro using the cytokinesis-blocked micronucleus assay in peripheral lymphocytes 24 h post-irradiation.

In addition, another set of blood samples were irradiated with the same modalities of the ADR exposure and cultured immediately after exposure ($T = 0$) to validate the RABiT-measured MNi 24 h post-exposure compared to the standard in vitro CBMN assay (Fenech 2007), in which samples are cultured from minutes to 1 h post-irradiation.

Donors

Whole blood was collected from twelve healthy volunteers (6 males and 6 females) at Columbia University Medical Center. The age range was between 26 and 46 years old. Informed consent was obtained from all volunteers according to IRB protocol. The donors were required to fill in an anonymous questionnaire to ensure that they had not been exposed to ionizing radiation in the previous 2 years before the blood draw in order to minimize the effect of ionizing radiation as a confounding factor. For each donor, 12 mL of blood was drawn by venipuncture into spray-coated sodium heparin (158 USP) vacutainer tubes (Becton–Dickinson and Company, Franklin Lakes, NJ). Blood samples were aliquoted into 1 mL samples and transferred to a centrifuge tube (50 mL volume); to each sample was added 3 mL of complete culture medium (RPMI 1640 +10 % FBS 1 % Pen/Strep; Invitrogen, Carlsbad, CA) without phytohemagglutinin (PHA). The contents were mixed gently, and the tubes were positioned in the irradiation chamber for radiation exposure.

Irradiation source and dosimetry

Sample irradiations were performed using the X-Rad 320 Irradiator (Precision X-Ray, North Branford, CT). For our studies, dose and dose rate were achieved by using a custom-made Thoraeus filter (1.25 mm Sn, 0.25 mm Cu, 1.5 mm Al). The filter provided a dose rate of 0.31 cGy/min (4.4 Gy for 24 h) at the maximum source to surface distance (SSD), 50 cm, for the low dose rate regime and 1.03 Gy/min at 40 cm SSD for the acute dose rate regime.

The X-Rad machine was calibrated using an N30013 ion chamber (PTW Farmer, Freiburg, Germany). During the actual irradiations, the delivery dose and the dose rate were monitored and measured in real time by a dose measuring parallel plate transmission chamber located inside in the filter holder assembly of the X-Rad machine. Doses of 0.56, 2.23 and 4.45 Gy were used for the acute and low dose irradiations.

Low dose rate experiments required the maintenance and exposure of blood samples for several hours under constantly controlled environmental conditions (37 °C, 5 % CO_2 and 80 % humidity). To fulfill this requirement, we built a custom incubator mainly made of plastic to avoid scattering radiation. Temperature was controlled through solid-state heaters on a feedback loop attached to the walls of the incubator to distribute the heat evenly. This setting maintained a temperature of 37 °C (±0.5 °C). The CO_2 concentration, humidity and temperature within the incubator were monitored using data loggers. Blood was exposed in 50-mL conical tubes angled to keep the samples within about a 20 cm diameter in order to minimize planar dose variation. The tube holder was rotated at speed of three rotations per hour to further minimize any dose inhomogeneity.

The ADR samples after irradiation were transferred to a CO_2 incubator and incubated for 24 h before processing.

Micronucleus assay

Irradiated blood sample was gently mixed, and for each sample, 2 mL of blood mixed with medium was transferred to culture flask and supplemented with extra fresh medium containing 2 % PHA for initiation of the culture. Cells were incubated for 44 h (37 °C, 5 % CO_2, 98 % humidity); following incubation, cytochalasin-B (Sigma-Aldrich, St. Louis, MO) at a final concentration of 6 μg/mL was added to block the cytokinesis after PHA stimulation.

Cells were harvested at 70 h. The contents of the flasks were transferred to a 15-mL centrifuge tube, and the tubes were centrifuged for 10 min at 1000 RPM to pellet the lymphocytes. Cells were treated with 0.075 M HCl solution at room temperature for 10 min and then fixed with ice-cold fixative (methanol/acetic acid 3:1).

The fixed cells were then stored in a fireproof fridge overnight and then moved to a −20 °C fireproof freezer. Prior to slide preparation, the lymphocytes were centrifuged and the supernatant discarded. The pellet was re-suspended with fresh fixative solution, and the lymphocyte suspension was dropped at the center of a microscope slide and spread by tilting the slide. The slides were allowed to air dry for 10 min before staining through the application of 50 μL of DAPI Vectashield mounting medium (Vector Labs, Burlingame, CA) and a cover slip. Slides were left overnight in the fridge prior to imaging.

Imaging and image analysis

Slides were imaged on a Zeiss epifluorescent microscope (Axioplan2 imaging MOT, Carl Zeiss, Germany) driven by MetaferMNScore software (MetaSystems, Althaussen, Germany). The MetaferMNScore automatically scans slides prepared for the cytokinesis-block micronucleus assay. Micronuclei in bi-nucleate cells were visually scored by the inspection of the cell gallery generated by the software. Each data point shown in Figs. 1 and 2 corresponds to the average of micronuclei frequencies obtained from 12 samples analyzed individually. For each sample, ~1000 binucleate cells were scored. Tables 1 and 2 show the micronuclei frequencies, the average and the SEM for each data point.

Statistics

Data obtained from the dose–response curve after ADR and LDR exposure for MNI scoring are presented as mean ± standard error of the mean (SEM).

Data for the ADR exposure of lymphocytes cultured at $T = 0$ and $T = 24$ h after exposure are presented as mean (±SEM) and compared by the two-tailed Student's t test indicating statistically no significant differences. The obtained dose–response curves were created and fitted using Excel (Microsoft Corp., Redmond, WA).

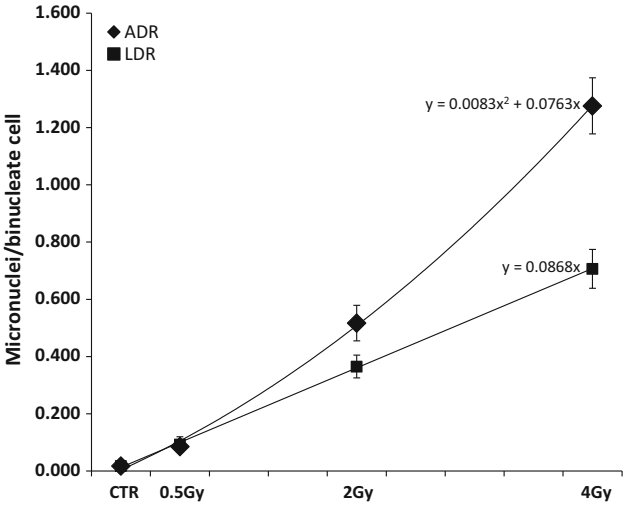

Fig. 1 Graph shows the RABiT-measured dose–response curve for micronuclei induction after X-ray irradiation administered with high dose rate (ADR) and low dose rate (LDR) modalities. The *bars* indicate the standard error of the mean

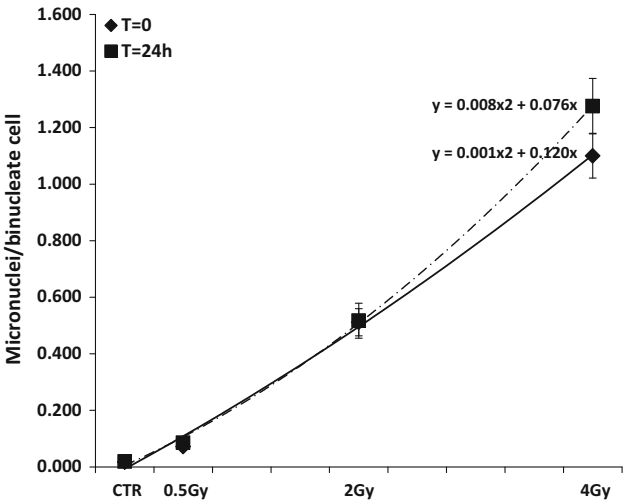

Fig. 2 Graph shows the RABiT-measured dose–response curves for micronuclei induction after X-ray irradiation delivered with high dose rate (ADR) and processed 24 h post-irradiation ($T = 24$ h) and within an hour post-irradiation ($T = 0$). The *bars* indicate the standard error of the mean

Results

Micronuclei frequencies were measured using the in vitro cytokinesis-blocked micronucleus assay, and the data are presented as micronuclei per binucleate cell (MNi/BN). Tables 1 and 2 show the average MNi frequencies measured and the SEM calculated for each data point.

Table 1 Micronuclei frequencies measured in samples exposed to graded doses of X-rays in both ADR and LDR scenarios

Donor	ADR experiment				LDR experiment			
	Dose				Dose			
	0 Gy	0.5 Gy	2 Gy	4 Gy	0 Gy	0.5 Gy	2 Gy	4 Gy
D1	0.027	0.039	0.116	1.514	0.008	0.054	0.121	0.192
D2	0.008	0.037	0.131	1.010	0.008	0.034	0.167	0.366
D3	0.032	0.115	0.571	1.072	0.036	0.089	0.401	0.812
D4	0.011	0.060	0.507	1.122	0.011	0.389	0.337	0.597
D5	0.029	0.104	0.715	1.491	0.029	0.089	0.388	0.707
D6	0.029	0.074	0.550	1.624	0.010	0.062	0.645	0.784
D7	0.012	0.116	0.62	0.98	0.010	0.066	0.41	0.718
D8	0.015	0.101	0.494	1.139	0.015	0.100	0.318	0.782
D9	0.019	0.097	0.855	1.603	0.019	0.075	0.523	1.077
D10	0.015	0.106	0.489	0.703	0.029	0.094	0.358	0.716
D11	0.011	0.095	0.672	1.875	0.014	0.078	0.351	0.906
D12	0.019	0.080	0.483	1.179	0.018	0.078	0.364	0.822
Average	0.019	0.085	0.517	1.276	0.017	0.101	0.365	0.707
SEM	0.002	0.008	0.062	0.098	0.003	0.027	0.040	0.068

The average frequencies and SEM calculated for each data point are also shown

Table 2 Micronuclei frequencies measured in samples exposed to graded doses of X-rays and cultured at $T = 0$ and $T = 24$ h post-irradiation

Donor	$T = 0$-h experiment				$T = 24$-h experiment			
	Dose				Dose			
	0 Gy	0.5 Gy	2 Gy	4 Gy	0 Gy	0.5 Gy	2 Gy	4 Gy
D1	0.014	0.030	0.029	1.324	0.027	0.039	0.116	1.514
D2	0.011	0.052	0.490	0.943	0.008	0.037	0.131	1.010
D3	0.034	0.099	0.602	0.896	0.032	0.115	0.571	1.072
D4	0.015	0.061	0.480	0.998	0.011	0.060	0.507	1.122
D5	0.016	0.089	0.550	1.147	0.029	0.104	0.715	1.491
D6	0.018	0.060	0.522	1.500	0.029	0.074	0.550	1.624
D7	0.026	0.083	0.60	0.93	0.012	0.116	0.62	0.978
D8	0.007	0.064	0.530	0.948	0.015	0.101	0.494	1.139
D9	0.011	0.090	0.728	1.494	0.019	0.097	0.855	1.603
D10	0.019	0.088	0.504	0.685	0.015	0.106	0.489	0.703
D11	0.012	0.078	0.597	1.440	0.011	0.095	0.672	1.875
D12	0.012	0.073	0.508	0.897	0.019	0.080	0.483	1.179
Average	0.016	0.072	0.512	1.101	0.019	0.085	0.517	1.276
SEM	0.002	0.006	0.048	0.079	0.002	0.008	0.062	0.098

The average frequencies and SEM calculated for each data point are also shown

Figure 1 shows the micronuclei frequencies in CBMN lymphocytes cultures after ADR and LDR irradiation.

The results show clearly that the yield of micronuclei decreases with decreasing dose rate starting at 2 Gy, whereas the response was indistinguishable from that to acute exposure in the low dose region, up to 0.5 Gy. We found a linear-quadratic dose–response relationship for the occurrence of micronuclei for the acute exposure and a linear dose–response relationship for the low dose rate exposure.

Figure 2 shows the micronuclei frequencies measured in human lymphocytes after ADR exposure when the cells were cultured immediately after exposure ($T = 0$) and 24 h post-irradiation ($T = 24$). The results show that for all the doses used no statistically significant differences in micronuclei frequencies were detected in the culture

conditions used after comparison with the two-tailed Student's t test (p values <0.01).

Discussion

The main thrust of this paper is the characterization of a high-throughput biodosimetry platform (RABiT) for dose reconstruction and risk assessment under mass-casualty scenarios such as an IND. In the present study, we analyzed the RABiT-measured in vitro dose–response relationship for micronuclei induction in human lymphocytes after acute and protracted X-ray irradiation. The scenario considered in this study is modeled after an IND event where it is estimated that the earliest organized emergency response will be capable of collecting samples at the earliest 24 h post-event from casualties inside the DFZ. Victims in these areas will be exposed to different dose rates due to their geographical position and sheltering conditions. Therefore, it is critical to characterize dose rate effects on the yield of MNi as well as the timing of sampling for the use of the RABiT system under a realistic concept of operations.

The results obtained showed that the micronuclei yield increases monotonically with the dose. While in the low dose region the yield of micronuclei remains essentially the same for both ADR and LDR, the results show clearly that for radiation doses higher than 2 Gy the yield of micronuclei decreases with decreasing dose rate. The ADR response has a linear-quadratic trend where the LDR response increases linearly with the dose.

To further characterize the RABiT-measured frequencies of micronuclei, the results obtained for the ADR 24 h post-irradiation were compared with the frequencies measured in samples cultured in the standard CBMN assay modality (samples processed within an hour post-irradiation: $T = 0$) using the same irradiation doses and setup. Two-tailed t test analysis showed that there were no statistically significant differences in the dose–response for each dose analyzed for both processing conditions. These results confirm the usefulness of the RABiT-measured micronuclei yield for dose reconstruction purposes as well as for DNA damage evaluation. The CBMN assay in peripheral blood lymphocytes is a well-established biological dosimetry tool for evaluation of radiation exposure and/or to evaluate the extent of DNA damage, for instance after an environmental, occupational or medical exposure. Because of its good reliability and reproducibility, the CBMN has become one of the standard cytogenetic techniques for genetic toxicology and in the field of radiation protection. The micronucleus assay has been thoroughly validated as a radiation biomarker in vivo in radiotherapy patients treated with large-field radiation as well in large-scale monitoring of nuclear power plant workers and hospital workers (Thierens and Vral 2009). An important advantage of the micronucleus assay is that the signal is stable for months after exposure, with a biological half-life of about 12 months, so the need for early acquisition of blood samples is removed (Thierens et al. 2005).

A large-scale radiological incident would result in an immediate critical need to assess the radiation doses received by thousands of individuals to allow for prompt triage and appropriate medical treatment. These persons might be exposed to substantial doses of ionizing radiations but may not show, at least initially, clear signs and symptoms of radio toxicity. Rapid assessment tools for immediate determination of absorbed dose will then be extremely helpful for screening and triage in case of a mass-casualty incident.

The authors believe that automating well-established bioassays represents a valid approach to high-throughput radiation biodosimetry both because a high throughput is achieved but also because, as we have demonstrated here, the RABiT can assess absorbed dose. These characteristics in addition to collection of data about geographical position and sheltering conditions of exposed individuals will allow the rapid screening/triage of people exposed to a variety of doses and dose rates.

This capability can be enhanced by the addition of exposed individual data about geographical location and sheltering condition allowing the rapid screening/triage of victims exposed to a variety of doses and dose rates.

References

Bhat NN, Rao BS (2003) Dose rate effect on micronuclei induction in cytokinesis blocked human peripheral blood lymphocytes. Radiat Prot Dosim 106(1):45–52

Boreham DR et al (2000) Dose-rate effects for apoptosis and micronucleus formation in gamma-irradiated human lymphocytes. Radiat Res 153(5 Pt 1):579–586

Coy SL et al (2011) Radiation metabolomics and its potential in biodosimetry. Int J Radiat Biol 87(8):802–823

DiCarlo AL et al (2011) Radiation injury after a nuclear detonation: medical consequences and the need for scarce resources allocation. Disaster Med Public Health Prep 5(Suppl 1):S32–S44

Fenech M (2006) Cytokinesis-block micronucleus assay evolves into a "cytome" assay of chromosomal instability, mitotic dysfunction and cell death. Mutat Res 600(1–2):58–66

Fenech M (2007) Cytokinesis-block micronucleus cytome assay. Nat Protoc 2(5):1084–1104

Fenech M (2010) The lymphocyte cytokinesis-block micronucleus cytome assay and its application in radiation biodosimetry. Health Phys 98(2):234–243

Garty G et al (2010) The RABIT: a rapid automated biodosimetry tool for radiological triage. Health Phys 98(2):209–217

Garty G et al (2011) The RABiT: a rapid automated biodosimetry tool for radiological triage. II. Technological developments. Int J Radiat Biol 87(8):776–790

Garty G et al (2015) An automated imaging system for radiation biodosimetry. Microsc Res Tech 78(7):587–598
Geard CR, Chen CY (1990) Micronuclei and clonogenicity following low- and high-dose-rate gamma irradiation of normal human fibroblasts. Radiat Res 124(1 Suppl):S56–S61
Goudarzi M et al (2014a) The effect of low dose rate on metabolomic response to radiation in mice. Radiat Environ Biophys 53(4):645–657
Goudarzi M et al (2014b) Development of urinary biomarkers for internal exposure by cesium-137 using a metabolomics approach in mice. Radiat Res 181(1):54–64
Hall EJ (1991) Weiss lecture. The dose-rate factor in radiation biology. Int J Radiat Biol 59(3):595–610
Jaworska A et al (2015) Operational guidance for radiation emergency response organisations in Europe for using biodosimetric tools developed in EU MULTIBIODOSE project. Radiat Prot Dosim 164(1–2):165–169
Knebel AR et al (2011) Allocation of scarce resources after a nuclear detonation: setting the context. Disaster Med Public Health Prep 5(Suppl 1):S20–S31
Kulka U et al (2015) Realising the European network of biodosimetry: RENEB—status quo. Radiat Prot Dosim 164(1–2):42–45
Laiakis EC et al (2014) Metabolic phenotyping reveals a lipid mediator response to ionizing radiation. J Proteome Res 13(9):4143–4154
Lyulko OV et al (2014) Fast image analysis for the micronucleus assay in a fully automated high-throughput biodosimetry system. Radiat Res 181(2):146–161
Marchetti F et al (2006) Candidate protein biodosimeters of human exposure to ionizing radiation. Int J Radiat Biol 82(9):605–639
Padovani L et al (1993) Cytogenetic study in lymphocytes from children exposed to ionizing radiation after the Chernobyl accident. Mutat Res 319(1):55–60
Paul S, Amundson SA (2008) Development of gene expression signatures for practical radiation biodosimetry. Int J Radiat Oncol Biol Phys 71(4):1236–1244
Pellmar TC, Rockwell S, G. Radiological/Nuclear Threat Countermeasures Working (2005) Priority list of research areas for radiological nuclear threat countermeasures. Radiat Res 163(1):115–123
Ramakrishnana N, Brenner D (2008) Predicting individual radiation sensitivity: current and evolving technologies. Radiat Res 170(5):666–675
Redon CE et al (2009) γ-H2AX as a biomarker of DNA damage induced by ionizing radiation in human peripheral blood lymphocytes and artificial skin. Adv Space Res 43(8):1171–1178
Repin M et al (2014) Next generation platforms for high-throughput biodosimetry. Radiat Prot Dosim 159(1–4):105–110
Rothkamm K et al (2013) Comparison of established and emerging biodosimetry assays. Radiat Res 180(2):111–119
Scott D, Hu Q, Roberts SA (1996) Dose-rate sparing for micronucleus induction in lymphocytes of controls and ataxia-telangiectasia heterozygotes exposed to 60Co gamma-irradiation in vitro. Int J Radiat Biol 70(5):521–527
Sorensen KJ et al (2000) The in vivo dose rate effect of chronic gamma radiation in mice: translocation and micronucleus analyses. Mutat Res 457(1–2):125–136
Swartz HM et al (2014) Comparison of the needs for biodosimetry for large-scale radiation events for military versus civilian populations. Health Phys 106(6):755–763
Thierens H, Vral A (2009) The micronucleus assay in radiation accidents. Ann Ist Super Sanita 45(3):260–264
Thierens H et al (2005) Cytogenetic biodosimetry of an accidental exposure of a radiological worker using multiple assays. Radiat Prot Dosim 113(4):408–414
Thierens H et al (2014) Is a semi-automated approach indicated in the application of the automated micronucleus assay for triage purposes? Radiat Prot Dosim 159(1–4):87–94
Turesson I (1990) Radiobiological aspects of continuous low dose-rate irradiation and fractionated high dose-rate irradiation. Radiother Oncol 19(1):1–15
Turner HC et al (2011) Adapting the gamma-H2AX assay for automated processing in human lymphocytes. 1. Technological aspects. Radiat Res 175(3):282–290
Vilenchik MM, Knudson AG (2006) Radiation dose-rate effects, endogenous DNA damage, and signaling resonance. Proc Natl Acad Sci USA 103(47):17874–17879
Voisin P et al (2001) The cytogenetic dosimetry of recent accidental overexposure. Cell Mol Biol (Noisy-le-grand) 47(3):557–564
Voisin P et al (2004) Criticality accident dosimetry by chromosomal analysis. Radiat Prot Dosim 110(1–4):443–447